



NODES

Nord Ovest Digitale E Sostenibile

NODES – Nord Ovest Digitale e Sostenibile

Report on the use of multi-source satellite images to the benefit of agriculture, on prediction models identified using temporal data acquired in other RM for resource optimization, and on optimization tools

SPOKE 6 - Primary Agroindustry

Flagship Project VINO – RM8

DELIVERABLE D8.2

Version history

| No. | Date | Details | Author(s) |
|-----|----------------|---------|---|
| 0.5 | June 2025 | | Dell'Acqua Fabio (Università di Pavia) |
| 1 | September 2025 | | Chiara Toffanin, Sohail Anwar (Università di Pavia) Paola Granillo (ERSAF) |

This document is part of the project NODES which has received funding from the MUR – Missione 4, Componente 2, Investimento 1.5 – Creazione e rafforzamento di “Ecosistemi dell'innovazione”, costruzione di “leader territoriali di R&S” – del PNRR funded by the European Union - NextGenerationEU with grant agreement no. ECS000000036



Table of Contents

| | |
|--|-----------|
| GLOSSARY..... | 4 |
| MULTI-SOURCE SATELLITE IMAGES..... | 5 |
| MULTI-SOURCE SATELLITE IMAGES DESCRIPTION | 5 |
| <i>The Dual-Polarimetric Radar Vegetation Index (DpRVI).....</i> | 5 |
| <i>Complementarity Between DpRVI and Optical Vegetation Indices.....</i> | 6 |
| <i>DpRVI and Biomass Estimation via Degree Days.....</i> | 7 |
| <i>Enhanced Spatial Insight with COSMO-SkyMed.....</i> | 7 |
| <i>Conclusion and Outlook.....</i> | 8 |
| <i>Publications.....</i> | 8 |
| PREDICTION MODELS..... | 9 |
| ABANDONED VINEYARDS DETECTION..... | 9 |
| <i>Methodology.....</i> | 9 |
| <i>Model Implementation & Hyperparameters.....</i> | 10 |
| <i>Model Evaluation.....</i> | 11 |
| <i>Result.....</i> | 11 |
| <i>Testing.....</i> | 13 |
| <i>Publications.....</i> | 13 |
| DETECTION OF GRAPEVINE FLAVESCENCE DORÉE | 14 |
| <i>Data and methods.....</i> | 14 |
| <i>Results.....</i> | 16 |
| <i>Discussion.....</i> | 23 |
| <i>References.....</i> | 23 |
| VIGOR MAPS GENERATED FROM UAV DATA | 24 |
| <i>Monitoring Vigor and Intra-Plot Variability.....</i> | 24 |
| <i>Vegetative Vigor Zones Interpretation.....</i> | 28 |

Glossary

| | Definition |
|--|---|
| Hub Coordinator (HC) | The Hub Coordinator represents the single point of contact for the implementation of the innovation ecosystem towards the MUR. It carries out the management and coordination activities of the innovation ecosystem, receives the fundings, verifies, and transmits to the MUR the reporting of the activities carried out by the Spoke and their affiliates. |
| National Recovery and Resilience Plan (NRRP) | This document uses the Italian acronym for the NRRP, which is PNRR (Piano Nazionale della Ripresa e Resilienza) |
| Research Program Manager | The person who will be responsible for the overall scientific contents of the NODES project. The NODES will appoint the Research Program Manager. It refers to “Responsabile del Programma di Ricerca” in the MUR’s Call of proposal for “Ecosistemi di Innovazione” |
| NODES’ Research and innovation program | NODES’ Research and Innovation program is articulated in specific programs for each Spoke, with the aim to promote and support applied research on topics consistent with the Intelligent Specialization Strategy, with the guidelines of the 2021-2027 partnership agreement scheme, with regional operational plans and regional and national research and innovation priorities. Although NODES’ Spokes are concentrated on different themes, they will organize their activities and actions within a common framework – NODES’ Booster Methodology |
| Spoke Coordinator | The University in charge of coordinating the Spoke’s ecosystem. It refers to “Spoke” in the MUR’s Call of proposal for “Ecosistemi di Innovazione” |
| Spoke Data Manager | The person who will be responsible for the monitoring and management of data generated at the Spoke level. The Spoke Coordinator will appoint the Spoke Data Manager. |
| Spoke Partner | The entity associated to the Spoke Coordinator. It can be an Innovation Cluster, Competence Center, Research Center related to the Spoke’s ecosystem and contributes to achieve objectives and impact under the Spoke’ leadership and management. It refers to “soggetti affiliati” in the MUR’s Call of proposal for “Ecosistemi di Innovazione”. |
| Spoke Project manager | The person who will be responsible for the management, coordination and progress of the project at the Spoke level. The Spoke Coordinator will appoint the Spoke Project Manager. |
| Spoke research and innovation program | NODES’ Research and Innovation program is articulated in specific programs for each Spokes. The spoke will leverage a consolidated collaboration with leading private and public companies and will focus the applied research activity on technological domains and applications that can favour the integration of SMEs into new value chains. |
| Spoke Scientific and Technical Manager | The person who will be responsible for the overall scientific contents of the project at the Spoke level. The Spoke Coordinator will appoint the Spoke Scientific and Technical Manager. |
| Spoke Stakeholders Committee (SC) | Consultation structure formed by relevant stakeholders (Government, universities, companies, civil society, third sector, etc.) |
| Spoke Thematic | General target focus and domain of the Spoke research. |
| Spoke Topics | Specific areas/lines of development within the Spoke. |
| Spoke Work Package Leader | At the Spoke level, Work Packages (WPs) will be organized by WP leaders, who will be responsible for performance evaluation and reporting. |
| Flagship Project | Main research project at the Spoke level with the goal of prototyping, testing, and demonstrating the research activities towards higher TRLs. |

Multi-source satellite images

Multi-source satellite images description

The integration of diverse satellite remote sensing data sources has become a cornerstone of precision viticulture. In regions like the Oltrepò Pavese hills of northern Italy, where vineyard structure, terrain orientation, and microclimatic variability create monitoring challenges, combining complementary observations from radar and optical sensors enables more robust agricultural assessments. This study, conducted within the framework of the PNRR-NODES project, leverages multi-source satellite imagery to analyze vineyard phenology, biomass evolution, and structural characteristics over a full growing season.

Three classes of satellite data were employed:

- Optical imagery from Sentinel-2, providing indices for detailed spectral information on vegetation health (e.g., NDVI, SVHI, LAI)
- Radar imagery from Sentinel-1, offering dual-polarimetric C-band backscatter information with frequent coverage
- High-resolution radar imagery from COSMO-SkyMed CSK constellation, capturing fine-scale spatial details at the cost of reduced revisit frequency and single-polarization (HH) measurements.

The synergy between these sources enhances our capacity to monitor vineyards throughout phenological phases, even under cloud cover or in conditions where optical data alone may be insufficient. The integration of these datasets facilitates not only temporal continuity but also improves the spatial precision of remote sensing analyses, especially when structural or orientation-based nuances influence canopy reflectance and backscatter patterns.

The Dual-Polarimetric Radar Vegetation Index (DpRVI)

The study conducted by Bergamaschi et al. (2025) pioneers the combined use of dual-polarimetric SAR data and optical imagery to characterize vineyard development, with a particular focus on the Dual-polarimetric Radar Vegetation Index (DpRVI). This radar-based index is leveraged as an innovative tool to monitor vineyard phenology, structural changes, and biomass dynamics over time.

The DpRVI is derived from Sentinel-1 C-band dual-polarimetric SAR data and calculated from the eigenvalue spectrum of the wave covariance matrix C_2 , specifically:

$$DpRVI = 1 - m\beta$$

where:

$$m = \frac{\lambda_1 - \lambda_2}{\lambda_1 + \lambda_2}, \beta = \frac{\lambda_1}{\lambda_1 + \lambda_2}$$

Alternatively, using the eigenvalue ratio $q = \frac{\lambda_2}{\lambda_1}$, it becomes:

$$DpRVI = \frac{q(q + 3)}{(q + 1)^2}$$

These formulations allow DpRVI to range from 0 (pure targets like bare soil) to 1 (random volume scatterers such as full-grown crops). This makes it particularly suitable for tracking the seasonal changes in vineyard canopy structure.

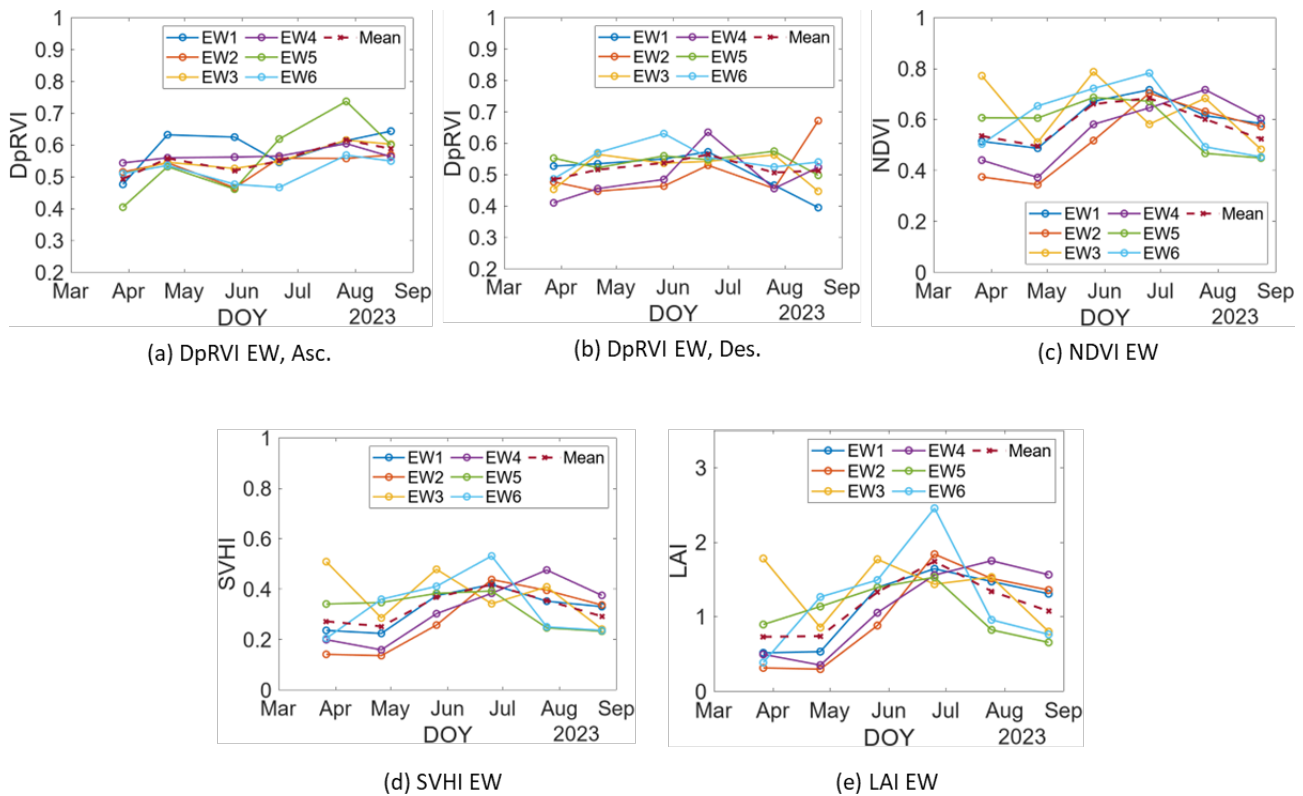


Figure 1. Behaviour, as a function of day of the year, of the vegetation indices for the East-West oriented vineyards

Complementarity Between DpRVI and Optical Vegetation Indices

Traditional optical indices like NDVI and SVHI measure vegetation greenness, relying on chlorophyll reflectance in the red and near-infrared bands. While useful, these indices are limited by atmospheric conditions and do not capture canopy structure. In contrast, DpRVI—insensitive to cloud cover—provides structural insight by responding to canopy geometry, dielectric properties, and surface roughness.

In the study, NDVI, SVHI, and LAI showed strong mutual correlation and followed a parabolic trend through the season, peaking in June. DpRVI presented a more gradual trend and weaker correlation with optical indices (Pearson's $r < 0.6$), confirming its independence and complementarity.

DpRVI and Biomass Estimation via Degree Days

Without ground-truth biomass data, the study used Cumulative Degree Days (CDD), also called the Winkler Index, as a proxy for growth, based on the concept that heat accumulation drives vine development. The formula used was:

$$GDD = \frac{T_{max} + T_{min}}{2} - T_{base}$$

Where $T_{base} = 10^{\circ}\text{C}$ for vineyards.

Biomass (BB) was then modeled using:

$$BB = k_{biom} \cdot \sqrt{CDD}$$

Given CDD increases roughly with the square of the day of year (DoY), biomass could be approximated linearly over time:

$$BB \propto DoY$$

DpRVI was plotted against CDD and showed a parabolic trend that mirrors biomass accumulation throughout the season.

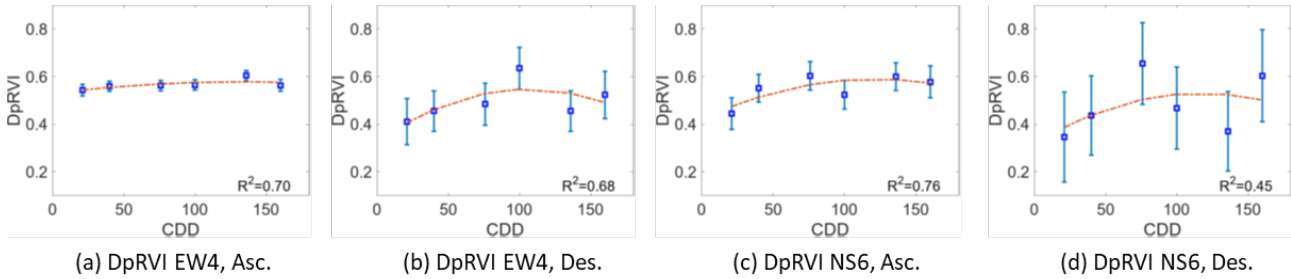


Figure 2. DpRVI evolution as a function of cumulative degree days for two sample vineyards: EW4, NS6.

Enhanced Spatial Insight with COSMO-SkyMed

To enrich the dataset, the study integrated radar data from COSMO-SkyMed, an X-band satellite constellation offering finer spatial resolution. Unlike Sentinel-1's 20 m resolution and dual-pol capabilities, COSMO-SkyMed operates in Stripmap Himage mode, providing 5 m resolution but only in single polarization (HH) and with lower temporal frequency.

Despite these limitations, COSMO-SkyMed's high spatial resolution yielded important benefits:

- Improved correlation with NDVI across the growing season.
- Higher sensitivity to vineyard row structures and canopy gaps, especially in early and mid-season.

The analysis showed that COSMO-SkyMed HH backscatter had higher correlation with NDVI than DpRVI, and this correlation increased consistently from May to August. This trend supports the hypothesis that spatial resolution plays a key role in accurately capturing vineyard characteristics, particularly when rows and inter-row spacing affect reflectance and backscatter

signals.

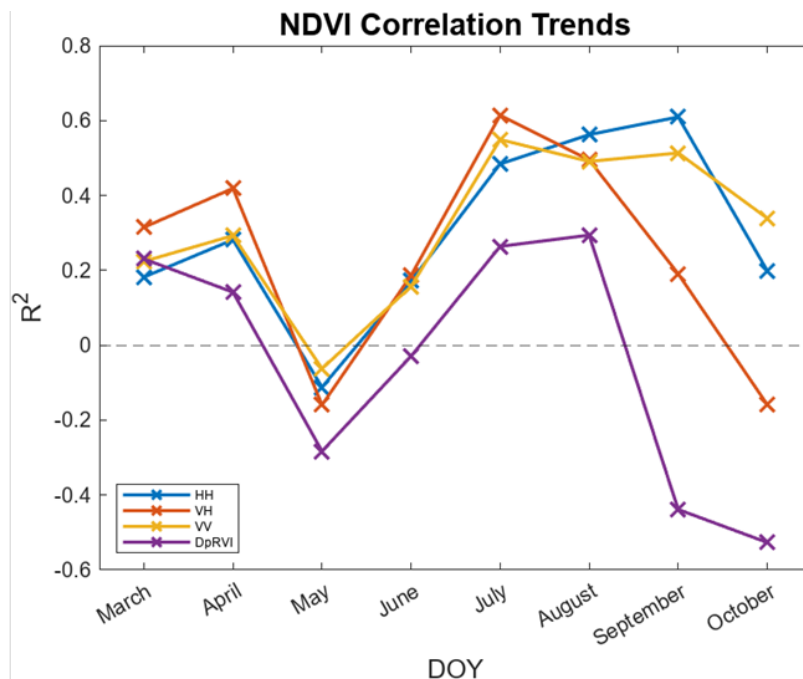


Figure 3. Correlation trend between COSMO-SkyMed HH backscatter and NDVI over time.

This outcome demonstrates that, even without polarimetric diversity, high-resolution SAR can outperform coarser radar indices in phenological correlation with optical data, reinforcing its value for vineyard monitoring.

Conclusion and Outlook

This study presents a novel joint application of Sentinel-1 DpRVI and COSMO-SkyMed HH backscatter with optical vegetation indices for vineyard monitoring. Key insights include:

- DpRVI captures structural vineyard traits independent of optical greenness.
- DpRVI temporal trends align with biomass accumulation modeled via cumulative degree days.
- COSMO-SkyMed's higher spatial resolution enhances correlation with NDVI, particularly during active growth phases.

These findings suggest that combining multi-source radar data with optical and phenological models can yield a comprehensive, resilient monitoring strategy for vineyards—one adaptable to cloud cover and capable of supporting sustainable, climate-informed viticulture.

Publications

- Bergamaschi, A., Verma, A., Bhattacharya, A., & Dell'Acqua, F. (2025). Joint Analysis of Optical and SAR Vegetation Indices for Vineyard Monitoring: Assessing Biomass Dynamics and Phenological Stages over Po Valley, Italy. IEEE Access.
- C. Garau, D. Marzi, M. Bordoni and F. Dell'Acqua, "Satellite Detection of Inter-Row Management Practices in a North-Italy Vineyard: Preliminary Results," IGARSS 2024 -

2024 IEEE International Geoscience and Remote Sensing Symposium, Athens, Greece, 2024, pp. 4325-4328, doi: 10.1109/IGARSS53475.2024.10641959.

- Andrea Bergamaschi, Abhinav Verma, Avik Bhattacharya and Fabio Dell'Acqua:
Spaceborne Monitoring of Vineyards: Optical and Multipolarized Radar-Based Indices
Tested on a Wine-Producing Area in Northern Italy in the Context of the Nodes Project,
TERRAENVISION 2025 Vol. 5 TNV-3424 Granada, Spain, 8-11 July 2025.

Prediction models

Abandoned vineyards detection

Climate change threatens viticulture in traditionally suitable regions. Grape quality, essential for good wine depends on proper management and suitable territories. In Northern Italy's Oltrepò Pavese region, enhancing wine production and economic stability for farmers is crucial. Moreover, detection of problematic vineyards is also a key point to enhance wine production. Abandoned vineyards harbour diseases whose control relies on insecticides and uprooting of infected vines, making abandoned vineyards persistent reservoirs of infection. Identifying such vineyards is challenging due to legal complications for owners. Since the phenomenon of vineyard abandonment or change of use is a practice that can lead to fines and penalties if not officially declared to the relevant authorities, the actual number of abandoned hectares is not known. This work aims to assist land management by suggesting areas of intervention to be monitored, as abandoned vineyards may be so for various reasons: abandonment due to lack of heirs, seasonal reduced vineyard control due to intense disease outbreaks and the impossibility of treatment, personal issues of the farm, excessive erosive phenomena that have temporarily made work impracticable.

Methodology

This study employs the YOLOv8 deep learning model to detect active and abandoned vineyards using orthophotos. YOLO (You Only Look Once) is a state-of-the-art object detection model which has gained popularity from its capabilities to work fast and accurately. YOLOv8 comprises three architectural components:

1. Backbone (CSPDarknet53 for feature extraction).
2. Neck (PANet for multi-scale feature fusion).
3. Head (anchor-free detection).

The model employs the Complete Intersection over Union (CIoU) loss function for bounding box regression:

$$L_{CIoU} = 1 - IoU + \frac{p^2(b, b^{gt})}{c^2} + av$$

where $p^2(b, b^{gt})$ is the Euclidean distance between predicted and ground truth boxes, c is the diagonal length of the minimum enclosing box, and v measures aspect ratio consistency.

A custom dataset was created from Google Earth Pro imagery of the Lombardy region in Italy, comprising 472 instances of abandoned vineyards and 410 instances of active vineyards collected from October (2014, 2015, 2018). Pre-processing techniques, including auto-orientation, static cropping with 25–75% horizontal and vertical regions, resizing to 640×640 pixels, and adaptive equalization for contrast adjustment, were applied to enhance image quality. Augmentation technique was also applied on the dataset to increase the overall dataset size to 1206 images for the training set, 51 images for validation and 50 images for testing set.

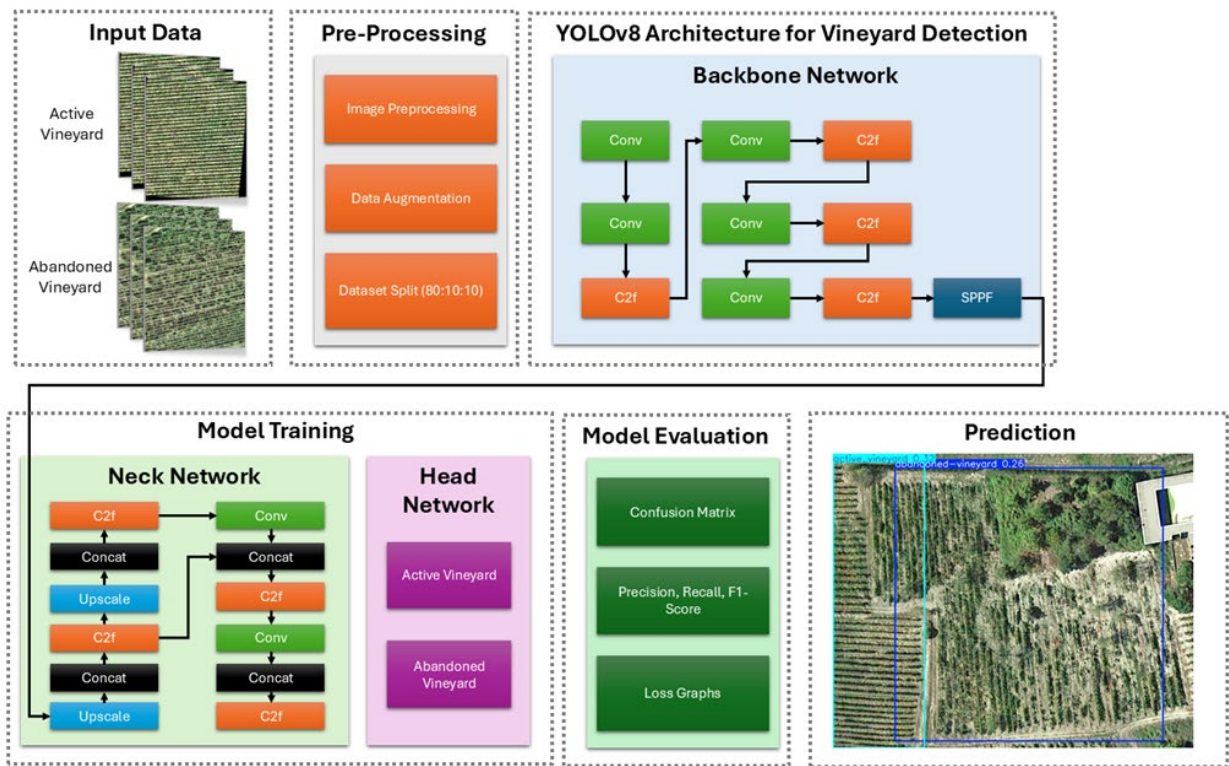


Figure 4. Block Diagram of the proposed methodology for abandoned vineyard detection

Model Implementation & Hyperparameters

The YOLOv8 model was employed for object detection utilizing pre-trained weight for comparison. The model was trained on the collected dataset as defined in the data.yaml configuration file. Each model was trained for 200 epochs with a varying batch size of 8, 16, 32 using images resized to 640 × 640 pixels. The model was trained on Google Collaboratory, an open-source cloud platform to run machine learning models with Tesla T4 GPU and CUDA version 12.4. All the hyperparameters defined in this section are performed for each YOLOv8 variant and batch size.

Adaptive learning rate strategy for optimization was adopted with initial learning rate (lr0) of 0.01, final learning rate (lrf) of 0.001, and momentum parameter value of 0.937 to achieve the optimal

balance between stability and speed of convergence. Weight decay (0.0005) was used to prevent overfitting with 3 epoch warmup phase is adopted to stabilise the model learning phase. Throughout inference, Non-Maximum Suppression (NMS) utilizing an IoU threshold of 0.7 was utilized in extracting detections and avoids redundant boxes. During training, model performance was checked continuously on a validation set (split = val) and metrics of performance like loss convergence and IoU were monitored. Training checkpoints were periodically saved, and the visualization tools were turned on to monitor the training progress. The experiment was carried out using Python (v3.11) combined with the Ultralytics YOLOv8 framework that uses PyTorch-based acceleration for (GPU-based) high-performance deep learning applications.

Model Evaluation

The proposed model was evaluated in terms of its ability to detect active and abandoned vineyards through a comprehensive set of metrics such as precision, recall, F1-score, confusion matrix, precision-recall curves, loss graphs.

Result

The results show the YOLOv8 model detects accurately active and abandoned vineyards, providing a reliable, systematic tool for vineyard management. Among the models tested, YOLOv8n (nano model) with 168 layers and 3 million parameters achieved optimal results with batch size of 32 shown in table 1. The model correctly classified 23 samples as abandoned vineyards, while misclassified 2 samples as active vineyards and 9 samples as background shown in figure 5. Similarly, for active vineyards, the model achieved 28 correct classifications but misclassified 3 samples as abandoned vineyards and 4 samples as background.

Table 1. Comparison of YOLOv8 variants with varying batch size

| Model | Batch Size | Class | Precision (Validation) | Recall (Validation) | Precision (Test) | Recall (Test) |
|----------------|------------|--------------------|------------------------|---------------------|------------------|---------------|
| YOLOv8n (nano) | 8 | Abandoned Vineyard | 0.948 | 0.733 | 0.891 | 0.579 |
| | | Active Vineyard | 1 | 0.891 | 0.935 | 0.788 |
| | 16 | Abandoned Vineyard | 0.833 | 0.833 | 0.884 | 0.632 |
| | | Active Vineyard | 0.899 | 0.926 | 0.959 | 0.788 |

| | | | | | | |
|------------------|-----------|---------------------------|--------------|--------------|--------------|--------------|
| | 32 | Abandoned Vineyard | 0.813 | 0.9 | 0.646 | 0.711 |
| | | Active Vineyard | 1 | 0.882 | 0.795 | 0.909 |
| YOLOv8s (small) | 8 | Abandoned Vineyard | 0.898 | 0.885 | 0.791 | 0.658 |
| | | Active Vineyard | 0.951 | 0.963 | 0.919 | 0.848 |
| | 16 | Abandoned Vineyard | 0.831 | 0.833 | 0.632 | 0.679 |
| | | Active Vineyard | 0.9 | 0.889 | 0.874 | 0.818 |
| | 32 | Abandoned Vineyard | 0.849 | 0.867 | 0.769 | 0.579 |
| | | Active Vineyard | 0.864 | 0.963 | 0.924 | 0.738 |
| YOLOv8m (medium) | 8 | Abandoned Vineyard | 0.913 | 0.704 | 0.663 | 0.62 |
| | | Active Vineyard | 0.814 | 0.889 | 0.933 | 0.847 |
| | 16 | Abandoned Vineyard | 0.861 | 0.824 | 0.694 | 0.553 |
| | | Active Vineyard | 0.92 | 0.926 | 0.905 | 0.867 |
| | 32 | Abandoned Vineyard | 0.798 | 0.8 | 0.749 | 0.706 |
| | | Active Vineyard | 0.818 | 0.996 | 0.788 | 0.895 |

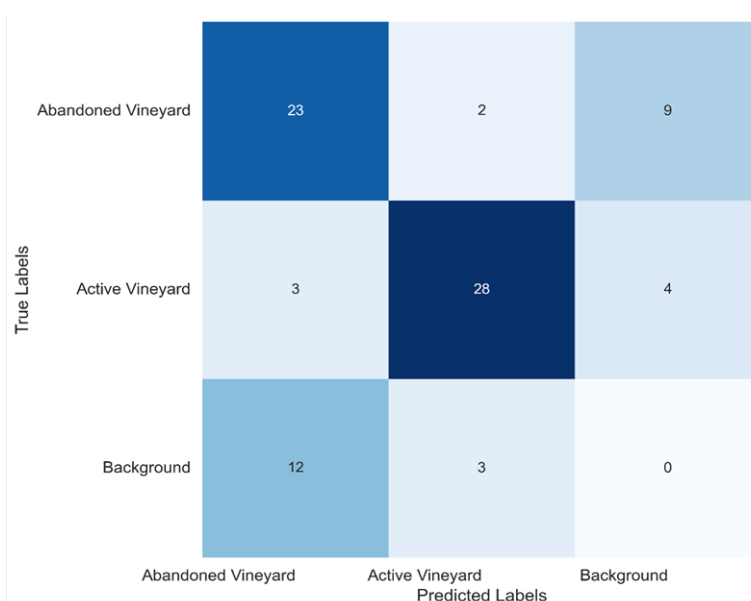


Figure 5. Confusion matrix on test set for abandoned vineyard detection

Testing

An example of the performance obtained on the test dataset is reported in Figure 6, where it is possible to see how the model is able not only to classify correctly the portion but also to detect and localize the areas of vineyard.



Figure 6. Active and abandoned vineyard detected by yolov8 (nano) 32 batch size model on test images.

The lightweight nature of YOLOv8 allows it to be deployed in edge computing environments, facilitating on-site vineyard monitoring without reliance on high-end cloud infrastructure. Unlike simple classification models, the YOLO-based detection system can simultaneously identify and locate multiple vineyards within a single image, eliminating the need for manual cropping and preprocessing. This approach addresses a critical gap in regional viticulture, aiding in the mitigation of disease spread and supporting sustainable agricultural practices. The research results proved that the proposed method has strong generalization and good detection performance for identifying vineyard abandonment using orthophotos and machine learning. This work can contribute as part of the economic stability and sustainability of wine grape production in Oltrepò Pavese.

Publications

- Anwar, S., Marchese, G., Toffanin, C., Vaglia, V.: Vineyard condition detection method using Google Earth Images and the YOLOv8 model in Northern Italy, EGU General Assembly 2025, Vienna, Austria, 27 Apr–2 May 2025, EGU25-981, <https://doi.org/10.5194/egusphere-egu25-981>, 2025.
- Anwar, S., Marchese, G., Vaglia, V., Toffanin, C.: Comparative Analysis of Yolo Models For Vineyard Abandonment Detection in Oltrepò Pavese, TERRAENVISION 2025 Vol. 5 TNV-3454 Granada, Spain, 8-11 July 2025.

Detection of grapevine flavescence dorée

This use case aims to identify and classify active foci of flavescence dorée (FD) in abandoned vineyards to support the prevention of its spread in productive vineyards. It integrates the outputs as previously discussed with satellite derived vegetation indices and soil moisture data.

In the literature, several articles report the use of optical sensors on *V. vinifera* plants for disease detection. For example, (Al-Saddik H, 2017) compares the effectiveness of different vegetation indices in recognizing areas affected by flavescence dorée. Others (Salvatore F. DI GENNARO, 2016) have studied the relationship between NDVI, acquired via remote sensing technologies, and FD-symptomatic plants monitored on the ground, obtaining promising results. One method for analysing this relationship is time series analysis. For the identification of FD-affected vineyards, methods that identify discontinuities in the time series considering both the seasonality of the time series and any trends, are of particular interest. In this use case we propose the Breaks For Additive Season and Trend (BFAST) algorithm as described by Verbesselt, Hyndman, Newnham, & Culvenor (2010) for this task. Once discontinuities are identified, we associate these with soil moisture content to rule out water stress as cause of the low NDVI values.

Data and methods

The study area comprises the area in Figure 7 with the abandoned vineyards as identified previously. Note that we choose to exclude the vineyards depicted by the blue circle to stay within one Sentinel-2 tile (tile 32TNQ). On the contrary we added the active vineyards of the company Riccagioia, as there was a known case of FD in July 2025. NDVI time series are calculated from cloud-masked Sentinel-2 images between January 2020 and October 2025, with a spatial resolution of 10x10m. To obtain clean time series, 16-day maximum composite images are created. A total of 441 NDVI measurements are in this way reduced to a time series of 86 NDVI composite images.

BFAST identifies discontinuities in time series, without the need to set a threshold or define a trajectory of change. First, the algorithm estimates the seasonal and trend components and the residual noise of the time series. Then the modelled time series is used for discontinuity identification (Verbesselt et al., 2010). The algorithm is run on each pixel that fully or partially covers one of the vineyards. The modelling period is ranging from 01-01-2022 to 30-04-2025 and the period for analysis ranges from 01-05-2025 to 08-10-2025. R^2 score is used to evaluate goodness-of-fit for the modelled NDVI timeseries. Models with scores below 0.6 are discarded. For the remaining pixels, pixels with an identified break or inspected. If the magnitude of the break is negative (hence, the obtained NDVI value is below the expected NDVI value based on the BFAST model), we flag the pixel as possibly infected by FD. Notably, there might be other causes for a drop in NDVI value. One of the causes we try to exclude is water stress. In this PoC,

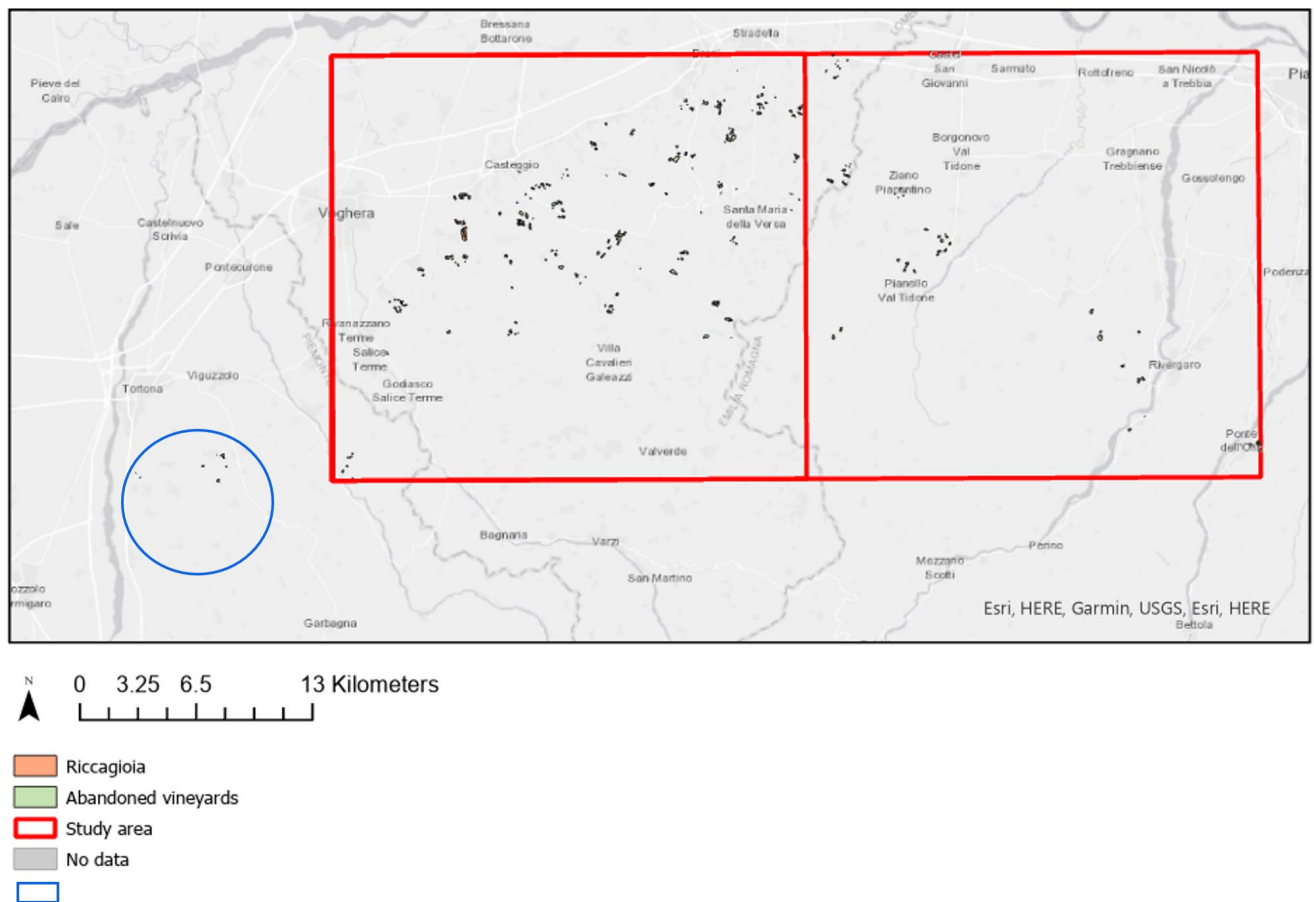


Figure 7. Area of interest (red) and abandoned vineyards (green). Added to the dataset are the active vineyards of Riccagioia, while the abandoned vineyards highlighted with the blue circle are removed from the dataset. As the vineyards are rather small in comparison to the study area, the results of this PoC will be divided into images, a western part and an eastern part, as evidenced by the division in the study areas bounding box.

we use surface soil moisture (SSM) to evaluate water deficit in vineyards. Surface soil moisture refers to the relative water content in the uppermost few centimeters of soil, indicating how wet or dry this layer is and is expressed as a percentage of saturation. We consider a value of SSM below 30% as critical. Therefore, if SSM is below 30% for 10 consecutive days, a drought deficit occurs (starting on the 11th day). Furthermore, if SSM remains below the 30% threshold for 20 consecutive days, the situation does not return to normal on the first day of a value $\geq 30\%$, only when this value persists for at least 5 days does this "reset" the situation to normal root water. We measure surface soil moisture with the Surface Soil Moisture – VI dataset from the Copernicus Land Monitoring Service (CLMS) portfolio (Copernicus, 2025), derived from satellite-based radar measurements. Measurements are available for the study area in irregular intervals of 1,4 or 6 days. In this use case, we assume that SSM remains stable between measurements.

Results

The entire study area has a total pixel count of 12.350.670, from which 32.302 pixels (partially) cover the vineyards under analysis. Roughly two-thirds of these pixels have an R^2 score below 0.6 ($n=21870$). These pixels cannot be used for further analysis. The remaining $n=10432$ pixels have R^2 scores ranging from 0.60 to 0.95, with a mean R^2 score of 0.76. Figure 8 shows some examples of measure and BFAST modelled NDVI time series and their R^2 score. The inset map comprises the Riccagioia vineyards with a known case of FD in July 2025. Figure 10 shows the classified R^2 score for the study area.

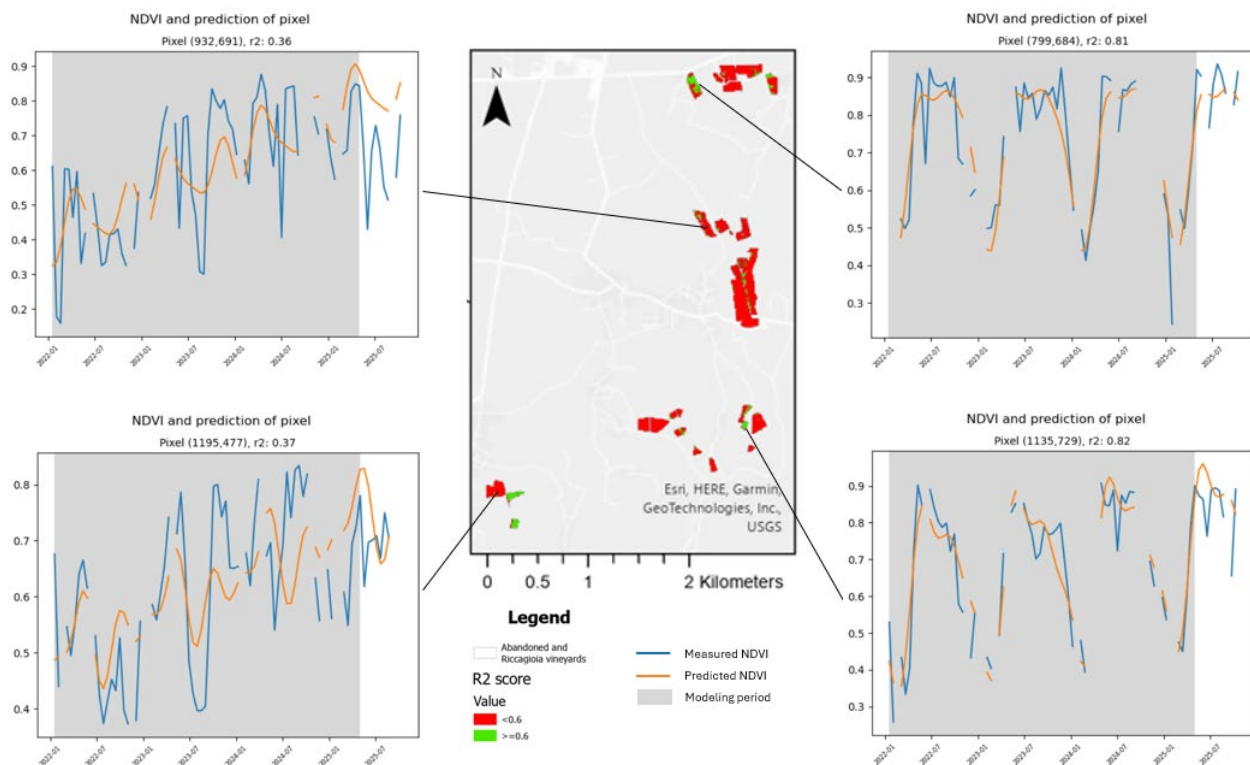


Figure 8. Examples of measured and predicted NDVI values. The graphs on the left show models with R^2 scores below 0.6 (0.36 and 0.37 respectively) and the graphs on the right show models with R^2 scores > 0.6 (0.81 and 0.82 respectively). The map in the middle shows the location of the pixels and the classification.

In 682 pixels out of the 10432 pixels with accepted R^2 score, a negative break is registered (hence, the NDVI time series shows a negative discontinuity). Two examples are shown in Figure 9, and the full map of the study area can be found in Figure 12. The pixels with a negative break are further analysed with respect to surface soil moisture. From the 682 pixels, 436 pixels are considered pixels with water deficit according to the rules described in the methodology (10 consecutive days with $SSM < 30\%$ or 20 consecutive days with $SSM < 30\%$ within 5 days recovery period). Hence, 246 pixels are showing a negative anomaly in the NDVI timeseries for which it cannot be attributed to a deficit in SSM (Figure 11).

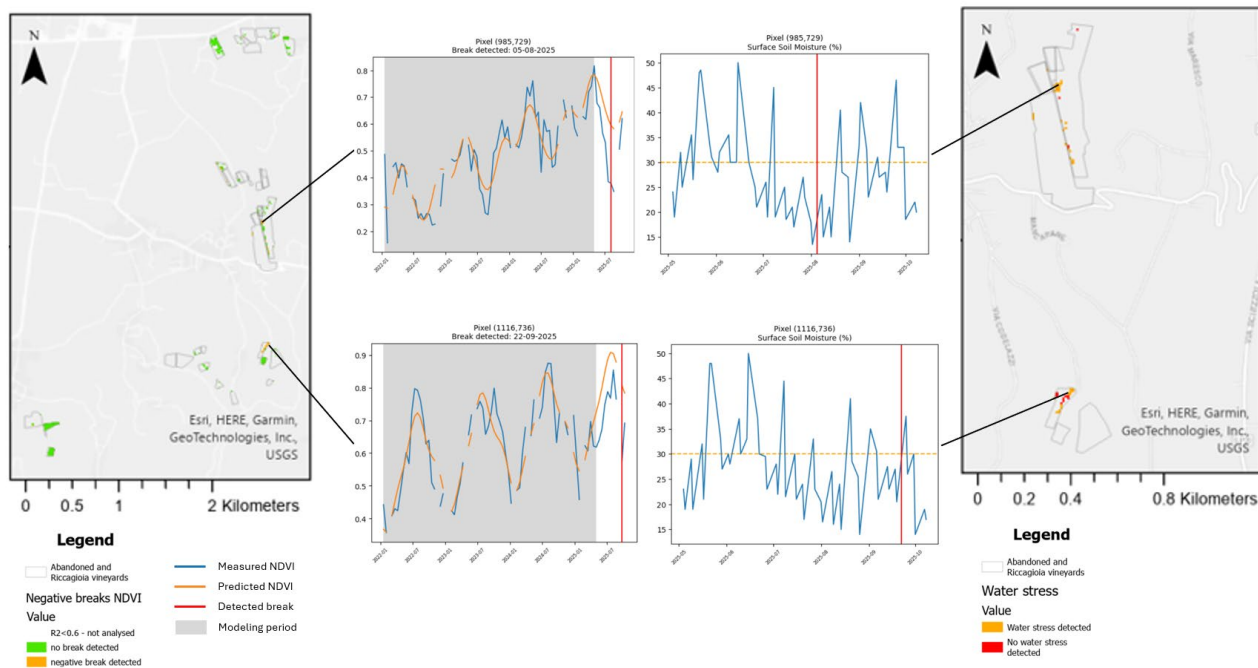


Figure 9. Examples of measured and predicted NDVI values with detected breaks. The break dates are respectively 05-08-2025 and 22-09-2025. Notice how the measured NDVI value drops far below the predicted NDVI value. The map on the left shows the location of the pixels and the classification. The graphs on the right side show the SSM time series with the detected break. Notice that both pixels are in water stress at time of the break (right side map), the risk class for the pixel is therefore medium.

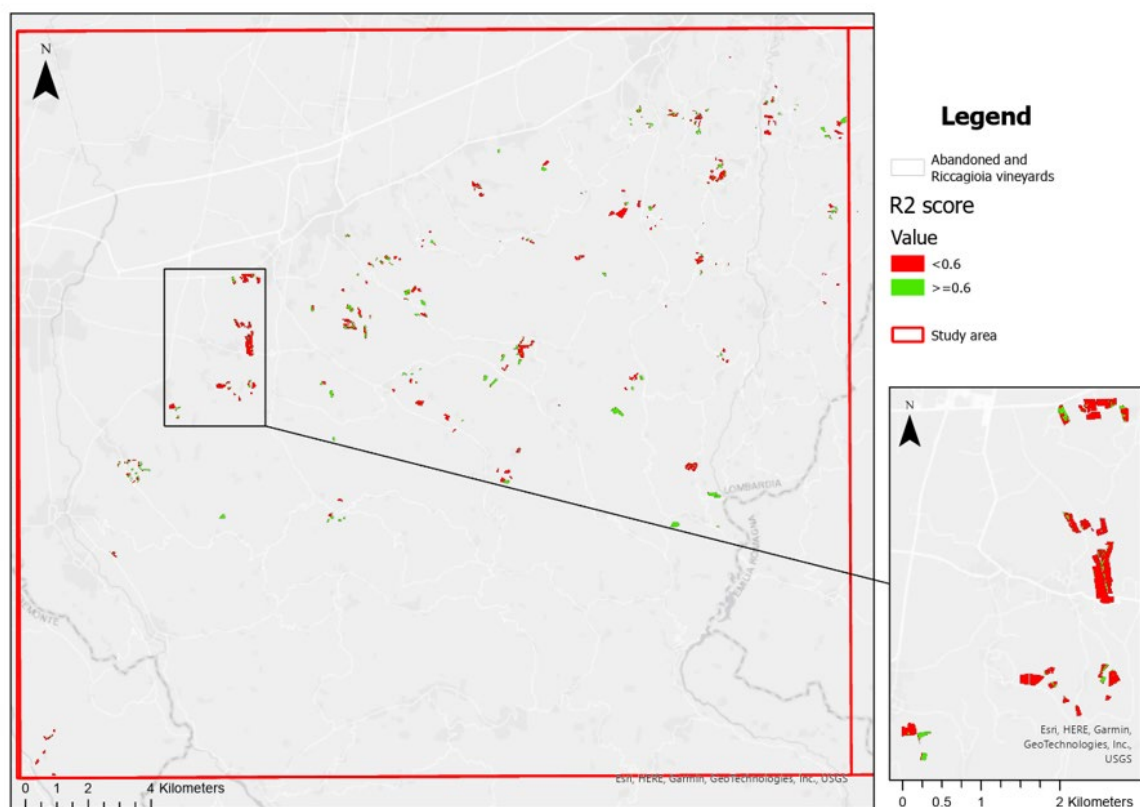
A final risk classification for the vineyards is based on the following criteria:

- High risk: a vineyard contains one or more (partial) pixels a negative anomaly in the NDVI timeseries and R^2 score ≥ 0.6 , no deficit in SSM is detected in the pixel.
- Medium risk: a vineyard contains one or more (partial) pixels a negative anomaly in the NDVI timeseries and R^2 score ≥ 0.6 , however, these anomalies can be attributed to a deficit in SSM.
- Low risk: a vineyard contains one or more (partial) pixels with R^2 score ≥ 0.6 , but no negative anomalies in NDVI timeseries are detected.
- No data: a vineyard contains only pixels with R^2 score < 0.6 .

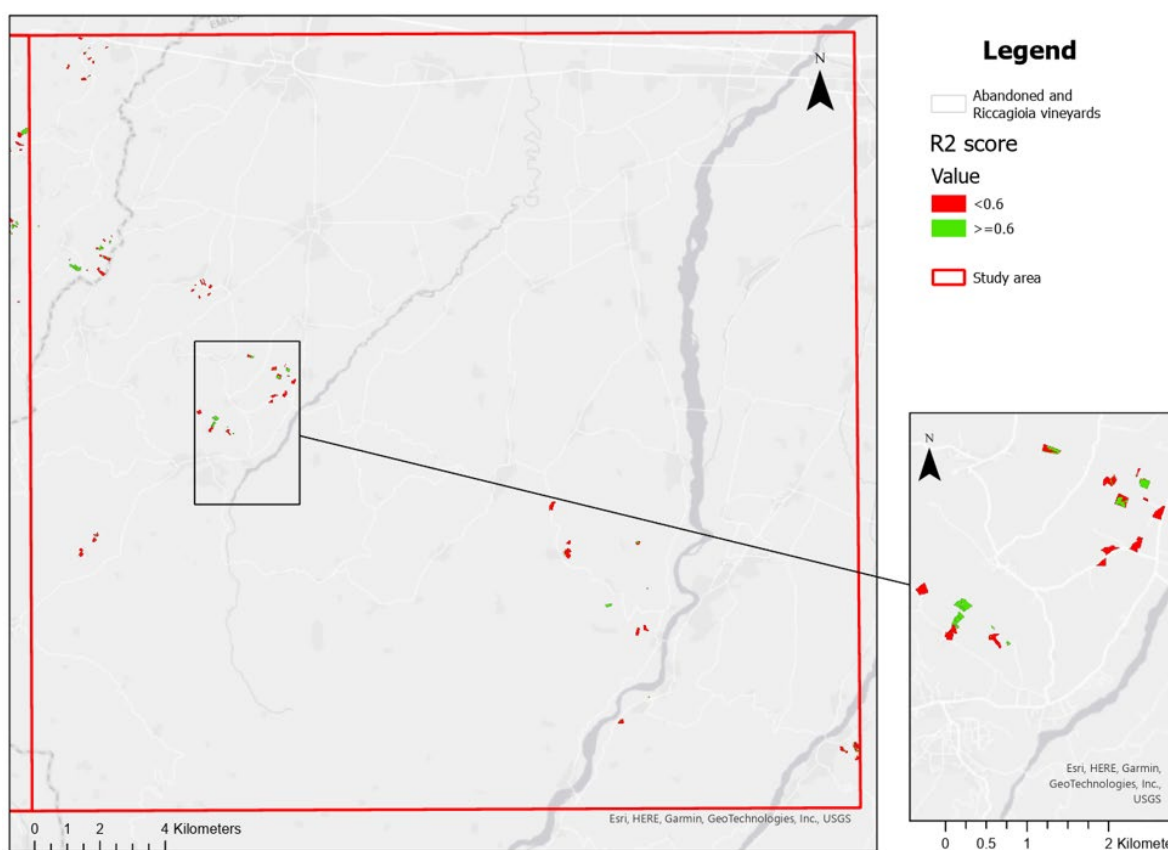
The results for each risk class are summarized in table 2 and Figure 13 shows the final risk map for the vineyards.

Table 2. Risk class distribution over pixels and vineyards

| Class | Description | Pixel count | Vineyards |
|-------------|--|-------------|-----------|
| No data | <ul style="list-style-type: none"> $R^2 < 0.6$ | 21.870 | 146 |
| Low risk | <ul style="list-style-type: none"> $R^2 \geq 0.6$ no negative break | 9750 | 210 |
| Medium risk | <ul style="list-style-type: none"> $R^2 \geq 0.6$ no negative break SSM < threshold cases | 436 | 37 |
| High risk | <ul style="list-style-type: none"> $R^2 \geq 0.6$ no negative break SSM > threshold cases | 246 | 35 |



a.



b.

Figure 10. Classified R^2 score. a. Western part of the study area. The in-set comprises the active vineyards of Riccagioia. b. for the western part of the study area.



Figure 11. Negative breaks in the NDVI time series as calculated with the BFAST algorithm. Only pixels with an R^2 score ≥ 0.6 were considered. a. Western part of the study area. b. Eastern part of the study area.

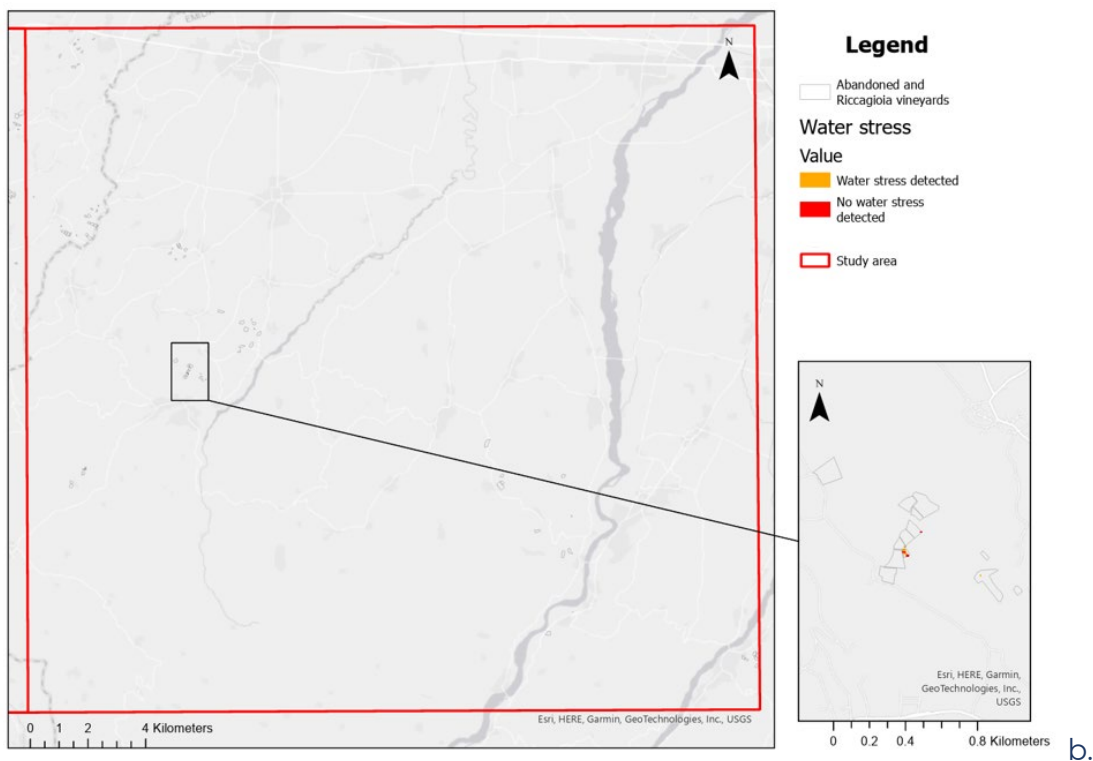
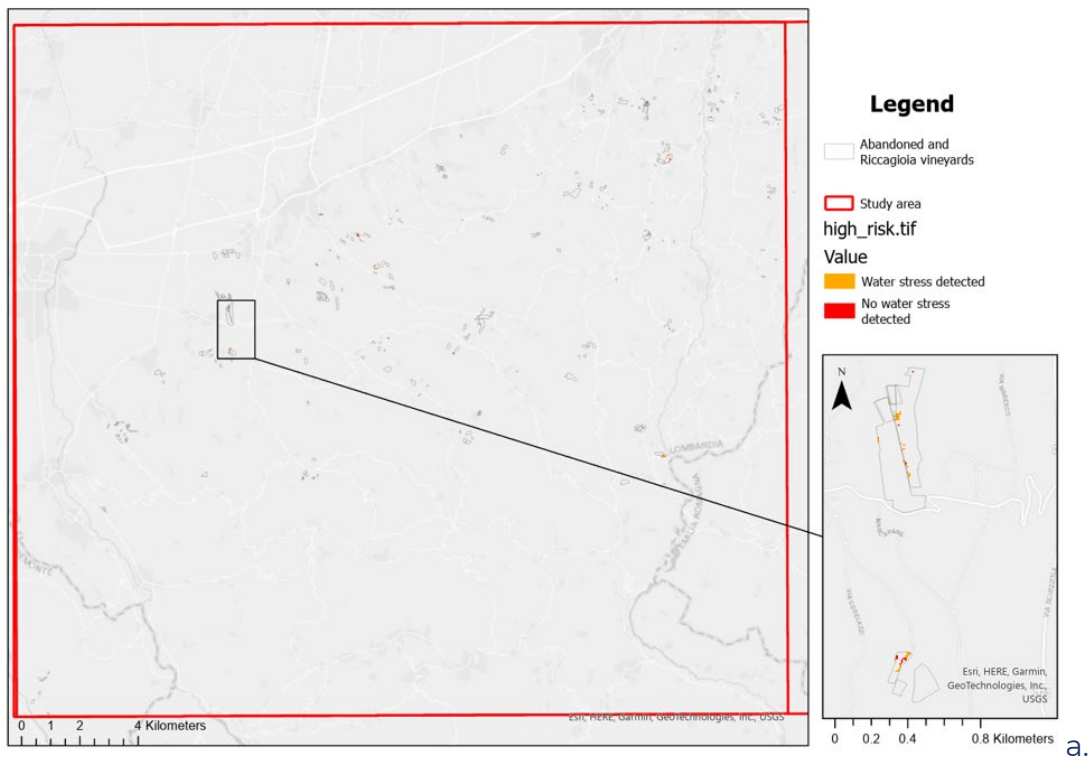


Figure 12. Water stress defined as SSM below 30% for 10 consecutive days or below 30% for 20 consecutive days, with a recovery period of 5 days. Only pixels with negative breaks in the NDVI time series and a R^2 score ≥ 0.6 were considered. Note that the zoom level of the in-set is adjusted to enhance visibility of the results. a. Western part of the study area. b. Eastern part of the study area.

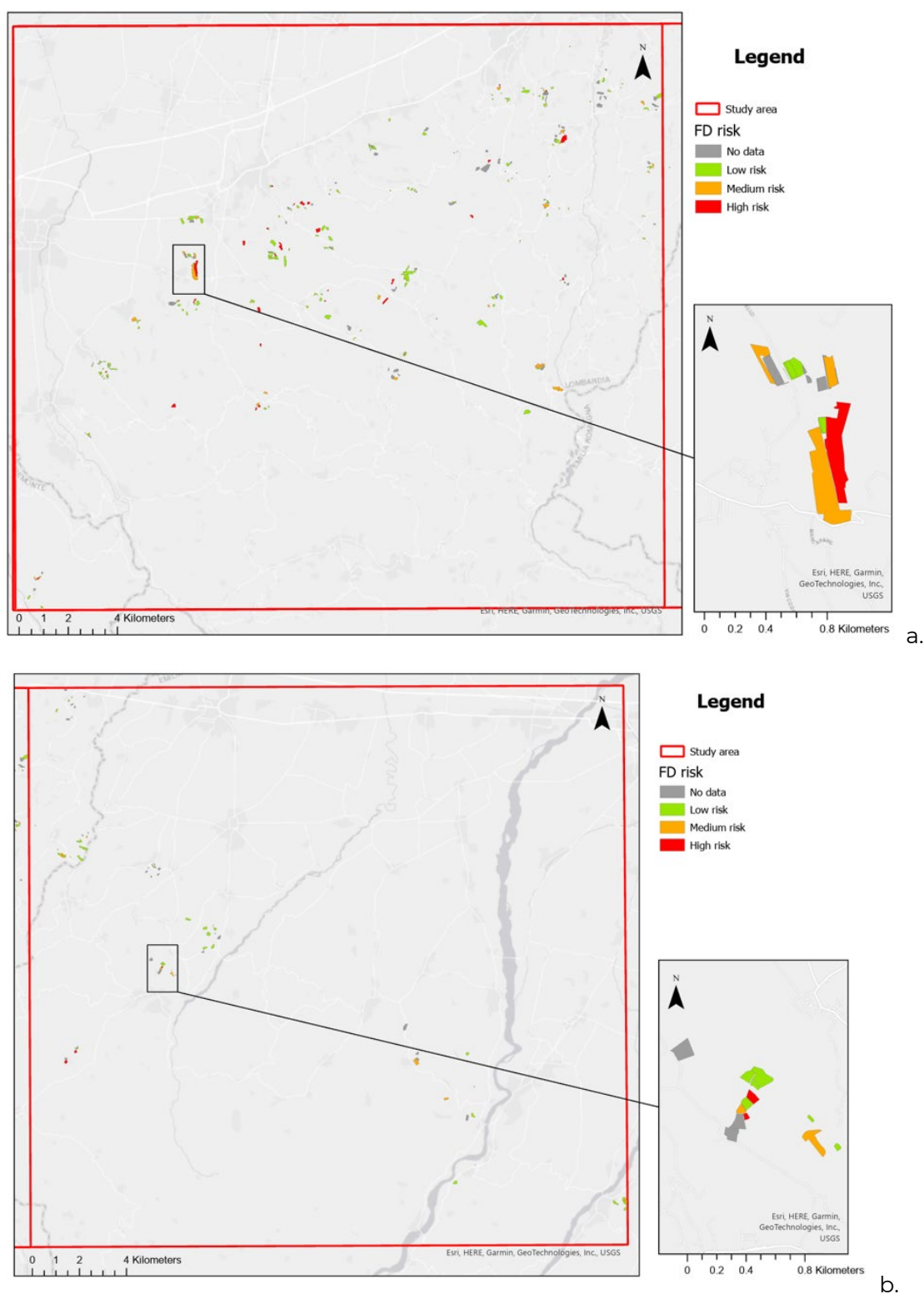


Figure 13. Flavescence Dorée (FD) risk. Vineyards are classified according to the maximum risk value in pixels (partially) covering the vineyard. a. Western part of the study area. The inset shows the active Riccagioia vineyards with a known cause of FD during the study period. Unfortunately, the exact field (and location) of the outbreak is unknown. b. Eastern part of the study area.

Discussion

This use case highlights the promising potential of using the location of abandoned vineyards to support the creation of a risk map for flavescence dorée (FD). By leveraging satellite-derived NDVI time series, the approach successfully identified negative anomalies in vegetation productivity, which were then cross-referenced with surface soil moisture (SSM) records to estimate FD risk levels. The initial modeling with BFAST provided a valuable starting point, with 32% of models achieving an R^2 score of 0.6 or higher. This sets a foundation for further optimization of model reliability. While daily SSM time series were not yet available, this phase demonstrated the feasibility of using existing data to approximate saturation dynamics. Upcoming work can incorporate higher-resolution temporal data to refine these assumptions and improve model sensitivity. Furthermore, next steps include the integration of additional environmental variables, such as temperature, humidity and vector spread in relation to wind speed and direction.

Validation remains a key area for advancement. Only one confirmed FD case was recorded during the study period, and outside the initial study perimeter, which underscores the importance of expanding the validation dataset. Targeted field campaigns and collaboration with vineyard operators can help pinpoint outbreak locations and provide critical ground truth data. Crucially, this field data can also be used to calibrate multi-parameter environmental indicators against confirmed cases of FD to improve the reliability and specificity of risk assessments. This will also support more confident exclusion of FD in vineyards showing negative NDVI breaks, ultimately contributing to more effective monitoring and early warning systems. In addition, the use of hyper-spectral and high-resolution satellite imagery, such as that expected from the upcoming IRIDE constellation, offers a promising avenue to enhance signal discrimination between grapevine vegetation and background elements like soil and understory growth. This will further improve the precision of anomaly detection and risk mapping in future deployments.

References

- Al-Saddik H, S. J. (2017). Development of Spectral Disease Indices for 'Flavescence Dorée' Grapevine Disease Identification. . National Library of Medicine. Sensors (Basel).
- Copernicus (2025) - CLMS Surface Soil Moisture – V1 dataset. Last accessed: 08-10-2025. DOI: <https://doi.org/10.2909/e934b15f-7d48-4c6d-a9c6-6484488aa58f>
- Salvatore F. DI GENNARO, E. B. (2016). Unmanned Aerial Vehicle (UAV)-based remote sensing to monitor grapevine leaf stripe disease within a vineyard affected by esca complex. *Phytopathologia Mediterranea*.
- Verbesselt, J., Hyndman, R., Newnham, G., & Culvenor, D. (2010). Detecting trend and seasonal changes in satellite image time series. *Remote Sensing of Environment*, 114(1), 106-115.

Vigor maps generated from UAV data

In the viticultural landscape of Northern Italy, characterized by a wide variety of microclimates and soils, the use of advanced monitoring technologies such as the NDVI (Normalized Difference Vegetation Index) is transforming vineyard management. This index, obtained through satellite or drone imagery, measures the "vigor" of vegetation—essentially the plant's ability to reflect near-infrared light compared to visible light—providing an estimate of vine health and photosynthetic activity.

Monitoring Vigor and Intra-Plot Variability

Knowing NDVI values allows winegrowers to precisely identify areas within the vineyard that show significant differences in vigor. This variability can be caused by factors such as water availability, soil fertility, disease presence, or environmental stress. Targeted interventions in these areas help optimize the use of resources like water, fertilizers, and phytosanitary treatments, reducing costs and environmental impact.

The service provided enables the creation of vegetation vigor maps based on the Normalized Difference Vegetation Index (NDVI), through the analysis and correlation of data from in-field sensors and multispectral surveys conducted with drones.

A total of five aerial surveys were carried out between June and September 2024, and six additional flights were conducted during the same period in 2026. These operations targeted four selected vineyards located in the Riccagioia area.

A management platform called Easy Farm is used and made available allowing users to view and download the material produced during the drone flight mission (reports, georeferenced data viewable on a map). The material is also available on GeoPortal.

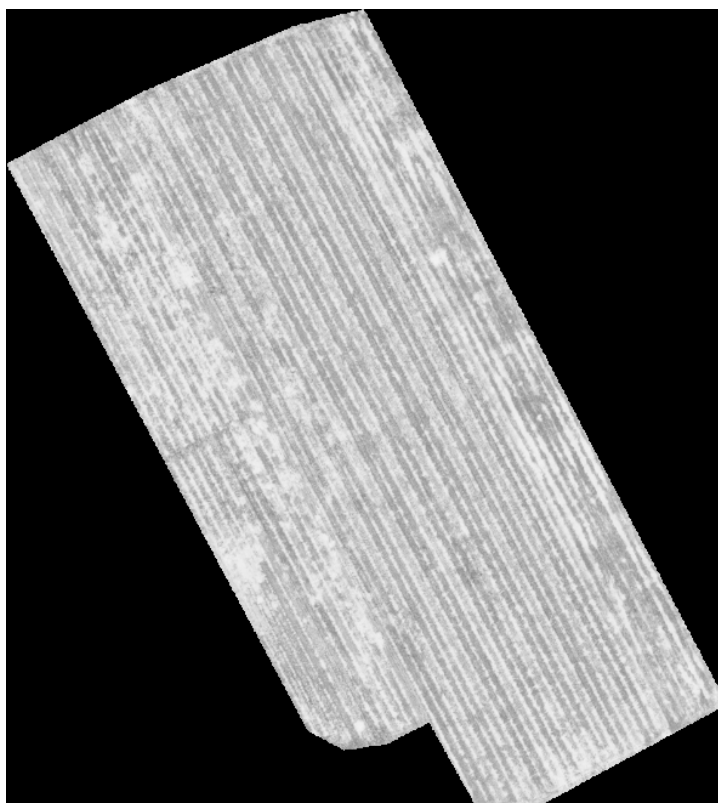
Drone-based surveys were conducted using equipment comparable in capability to the DJI Matrice 100 and Phantom 4 Pro, equipped with Agrowing and Mapir multispectral cameras. These instruments enabled the generation of NDVI maps, which provide a rapid and intuitive assessment of crop physiological status.



The NDVI maps are derived from the differential reflection of specific light spectrum frequencies on the plant canopy, offering insights into vegetation vigor and potential stress conditions.

The index is easy to interpret: NDVI will be a value between -1 and 1. An area with nothing growing in it will have an NDVI of zero. NDVI will increase in proportion to vegetation growth. An area with dense, healthy vegetation will have an NDVI of 1. NDVI values less than 0 suggest lack of dry land. An ocean will yield an NDVI of -1.

An example output from the drone survey is presented below, specifically the NDVI map of Vineyard No. 4, obtained during the initial field flight conducted in early June.

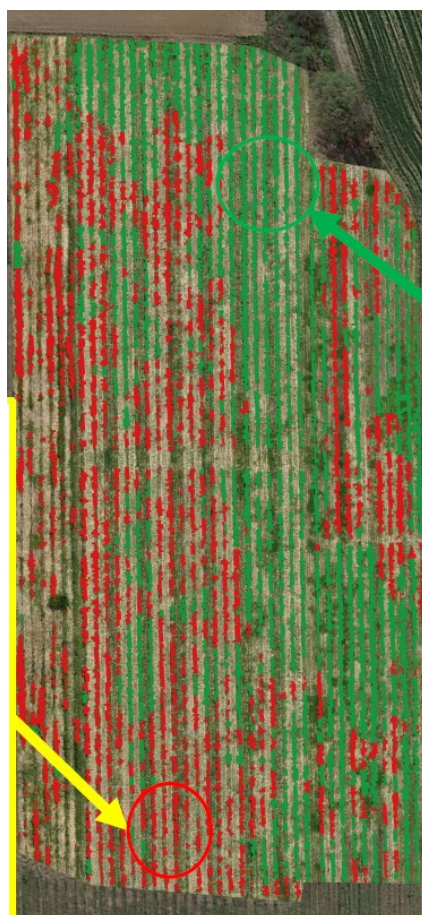
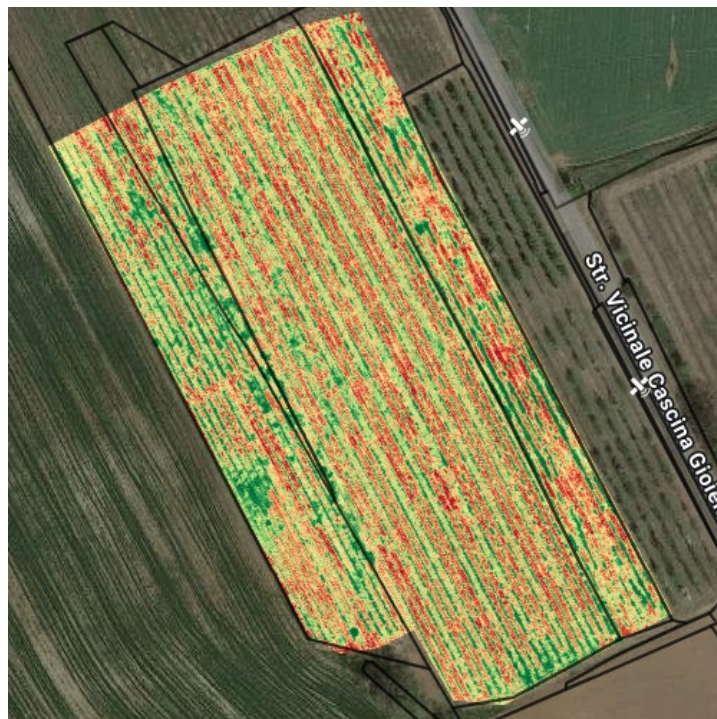


NDVI map of Vineyard No. 4



NDVI map of Vineyard No. 4

By integrating and analyzing the collected data, and with the support of agronomic consulting, it was possible to produce detailed reports such as the one shown in the figures below.



Vegetative Vigor Zones Interpretation

The green zones indicate areas of high vegetative vigor, characterized by:

- Plants exhibiting strong productive potential.
- A well-developed and dense canopy structure.
- Adequate availability of nutritional and water resources, supporting optimal physiological development.

In contrast, the red zones represent areas of low vegetative vigor, where:

- Plants show limited or absent productive capacity.
- The canopy is poorly developed or entirely missing.
- Nutritional and water resources are insufficient to sustain proper growth. These conditions may be attributed to soil characteristics, particularly low water retention capacity.

All flight operations were carried out by professional pilots certified by ENAC (Ente Nazionale per l'Aviazione Civile), ensuring compliance with national aviation regulations and operational safety standards.

In addition to aerial data acquisition, the study incorporated information from pre-installed in field sensors. The integration and correlation of these datasets allowed for a more comprehensive analysis of crop conditions, enhancing the reliability and granularity of the results.

Finally, expert agronomic consulting was employed to support the interpretation of the collected data. This step was essential for translating remote sensing outputs into actionable insights for precision agriculture and informed decision-making.